Preprinted version of the Fully 3D Proceeding Paper
Copyright by the Fully3D committee

Image Artifact Influence on Motion Compensated Tomographic Reconstruction in Cardiac C-arm CT

Kerstin Müller, Chris Schwemmer, Günter Lauritsch, Christopher Rohkohl, Andreas Maier, Hein Heidbüchel, Stijn De Buck, Dieter Nuyens, Yiannis Kyriakou, Christoph Köhler, Rebecca Fahrig, and Joachim Hornegger

***Abstract*—In C-arm CT, electrocardiogram (ECG)-gating of data from a single C-arm rotation provides only a few projections per heart phase for image reconstruction. This view starvation leads to prominent streak artifacts and a poor signal to noise ratio. Motion compensation techniques allow for the use of all acquired data for image reconstruction. Cardiac motion can be estimated by deformable 3-D/3-D registration processed on initial 3-D images of different heart phases. The initial 3-D images are computed from the few, ECG-gated data. In this paper, the sensitivity of the 3-D/3-D registration step to the image quality of the initial images is studied. Different reconstruction algorithms are evaluated for a recently proposed cardiac C-arm CT acquisition protocol. An iterative few-view reconstruction, and a filtered backprojection method (FDK) with and without a bilateral filter are investigated with respect to the final motion compensated reconstruction quality. The algorithms were tested on a phantom and on a porcine model using qualitative and quantitative measures. The phantom projection data and geometry is publicly available and can be downloaded from conrad.stanford.edu/data/heart. The results show minor differences between the three motion compensated reconstructions. For two heart phases a relative root mean square error (rRMSE) of $\approx$ 0.09 and 0.06 and an universal image quality index (UQI) of $\approx$ 0.98 and 0.99 was achieved. The motion compensated reconstructions that use all of the projection images show a clear improvement compared to the initial reconstructions. Given the relatively small differences in final image quality, the algorithm of choice is likely to be the one with smallest computational complexity.**

I. Introduction

A. Purpose of this Work

Today, an angiographic C-arm CT system is standard in interventional cardiology laboratories. By acquiring a set of 2-D high-resolution X-ray images from various directions a 3-D image can be computed. Due to the long acquisition times of several seconds, 3-D imaging of moving objects such as the heart is still an open problem. Commonly, an electrocardiogram (ECG) signal is recorded synchronous with the acquisition and a relative heart phase can be assigned to each projection. In order to improve temporal resolution, the reconstruction can be performed with the subset of the projections that lie inside a certain ECG window centered at the favored heart phase [1]. However, the available number of projections is insufficient for imaging of the heart chambers. Streak artifacts hamper the use of the reconstructed volumes. One possible solution is the use of all acquired projection data in combination with compensation for the cardiac motion in the reconstruction step. The cardiac motion can be estimated by registration of initial 3-D volumes of each heart phase to one reference heart phase. The goal of this paper is to find a suitable reconstruction algorithm for the initial 3-D volumes that can provide image quality sufficient for 3-D/3-D registration.

K. Müller, C. Schwemmer, A. Maier and J. Hornegger are with the Pattern Recognition Lab, Department of Computer Science and the Erlangen Graduate School in Advanced Optical Technologies (SAOT), Friedrich-Alexander-Universität Erlangen-Nürnberg, Erlangen, Germany. email: kerstin.mueller@cs.fau.de. C. Rohkohl, G. Lauritsch, Y. Kyriakou and C. Köhler are with the Siemens AG, Healthcare Sector, Forchheim, Germany. H. Heidbüchel, S. De Buck and D. Nuyens are with the Department of Cardiovascular Sciences, University of Leuven, Leuven, Belgium. R. Fahrig is with the Department of Radiology, Stanford University, Stanford, CA, USA. The authors gratefully acknowledge funding support from the NIH grant R01 HL087917 and of the Erlangen Graduate School in Advanced Optical Technologies (SAOT) by the German Research Foundation (DFG) in the framework of the German excellence initiative.

B. State-of-the-Art

Motion estimation is already investigated in the area of CT imaging. Cardiac motion is calculated by using 3-D/3-D registration of initial images. The deformation of the heart between heart phases is computed by various optimization algorithms. The individual algorithms differ in the objective function, constraints and optimization techniques [2],[3]. In C-arm CT the reconstruction of initial images at different heart phases with projection data acquired during one single C-arm sweep is still an unsolved problem. The reconstruction quality of the initial images is highly dependent on the choice of the acquisition protocol. In recent studies, an image acquisition of multiple-sweeps of the C-arm is used [1], [4]. The number of gated projection images increases and few-view artifacts are avoided. Techniques of 3-D/3-D registration can be applied to estimate the cardiac motion. However, the longer imaging time results in a higher contrast burden and radiation dose for the patient. Therefore, a new protocol for cardiac C-arm CT was presented [5]. It is a single sweep protocol with 10 - 15 s scan time. The quality of the reconstructed images is still critical, even when using compressed sensing algorithms [6]. In this paper, we investigate whether initial images might be generated from this protocol that are of sufficient quality for cardiac motion estimation.

II. Methods and Materials

A. Initial 3-D Image Generation

1) ECG Selection: The ECG-gating is performed by inserting a weighting function with respect to the relative heart phase into the standard FDK approach. The weighting function is centered at a specific heart phase and has the shape of a cosine or rectangular window [7]. Here, we use a strict rectangular gating function of minimal width, i.e. only one view per heart cycle is considered. A certain number H of volumes $f_h(\boldsymbol{x})$, with $h = 1, \ldots, H$ at specific heart phases are reconstructed. Every heart phase h corresponds to a relative heart phase of $[0\%, \ldots, 100\%]$ between two successive R-peaks[1].

2) 3-D Image Reconstruction:

a) ECG-gated Filtered Backprojection Volume Reconstruction (FDK-VR): For this approach, the volumes are reconstructed with a FDK reconstruction algorithm. The ECG-gated FDK images are highly corrupted by noise and have severe streak artifacts.

b) Filtered ECG-gated Filtered Backprojection Volume Reconstruction (FFDK-VR): The FDK-VR volumes in paragraph II-A2a are filtered by a 3-D bilateral filter [8] to reduce the streak artifacts and eliminate noise. The edge-preserving bilateral filter can be applied due to the high contrast inside the heart chambers compared to the streak artifacts.

c) Few-view Volume Reconstruction (F-VR): Images are reconstructed with an iterative few-view reconstruction algorithm that considers the sparse sampling condition. Here, the prior image constrained compressed sensing (PICCS) and the improved total variation (iTV) algorithm are used [9], [10]. The optimization is performed iteratively with a gradient descent scheme and with the same parameters as described in [6]. The resulting volumes have fewer streak artifacts, but are smoother than a standard non-gated FDK reconstruction.

B. Motion Field Estimation via 3-D/3-D Registration

For cardiac motion estimation, one heart phase needs to be selected as reference phase. The corresponding volume is called reference volume and all other volumes are registered to the reference volume. In this paper, a toolbox for nonrigid registration of medical images called `elastix` is used for the 3-D/3-D motion estimation [11]. Here, the deformable registration is based on a uniform cubic B-spline. A multi-resolution scheme of 4 levels is used with a sampling factor of 2 on each pyramid level. A number of $c = 16$ control points in each dimension are used at the highest image resolution. The negative normalized cross correlation (NCC) is used as the objective function and is minimized with an adaptive stochastic gradient descent optimizer. Empirical experiments showed that 500 iterations on each pyramid level are sufficient to result in a minimal objective function value. In order to restrict the motion vector field to a certain region of interest (ROI) where the heart motion is expected, a motion mask delimits the motion. In this first implementation the mask volume is generated manually by the user.

C. Motion Compensated Reconstruction

For final image reconstruction, motion is compensated using Schäfer's method [12]. The resulting volumes are denoted by the type of ECG-gated volume reconstruction with the subscript r (FDK-VR$_r$, FFDK-VR$_r$, F-VR$_r$,).

III. Experiments

A. Phantom Model

The presented 3-D/3-D registration approach has been applied to a ventricle data set comparable to the XCAT phantom [13], [14]. It is assumed that all materials have the same absorption behavior as water. The bloodpool density of the left ventricle was set to 2.5 g/cm^3, the density of the myocardial wall to 1.5 g/cm^3 and the blood in the aorta to 2.0 g/cm^3. We simulated data using a clinical protocol with the same parameters as for the porcine model presented in the following Section III-B. Poisson distributed noise was added to the simulated projections such that the noise characteristic of the reconstructed image fits to that of the clinical data. The phantom projection data and geometry is publicly available and can be downloaded from conrad.stanford.edu/data/heart.

B. Porcine Model

The methods were also applied to an experimental data set of a porcine model. Image acquisition was performed using an Artis zee system (Siemens AG, Healthcare Sector, Forchheim, Germany). The acquisition time was 14.5 s capturing 381 projection images with 30 f/s, and an angular increment of 0.52° during one C-arm sweep [5]. The isotropic pixel resolution was 0.31 mm/pixel (0.19 mm in isocenter) and the detector size 1240 × 960 pixel. The heart rate was synchronized with the framerate of the imaging acquisition through external heart pacing to 131 bpm. A total of 32 images per heart cycle are acquired resulting in a number of reconstructed heart phases $H = 12$. A volume of ~ 150 ml contrast fluid was administered intravenously at a speed of 10 ml/s beginning 5 s before the X-ray rotation was started. Image reconstruction was performed on an image volume of (25.6 cm)^3 distributed on a 256^3 voxel grid.

IV. Results and Discussion

A. Complexity Analysis

The three approaches (Section II-A2) have different computational complexity. The most complex part for the FDK-VR is the backprojection step with a complexity of $\mathcal{O}(N \cdot n^3)$, with n the side length of the volume and N the number of projections. The backprojection is performed on the GPU. The FFDK-VR utilizes the FDK-VR and additionally performs a filtering step. The used bilateral filter is implemented in a straightforward manner on the GPU and has a complexity of $\mathcal{O}(n^3 \cdot r^3)$, where r denotes the filter size ($r = 5$ in this paper). Most parts of the PICCS+iTV algorithm are implemented on the GPU, but the runtime of the iterative F-VR reconstruction algorithm still exceeds the FDK-VR and FFDK-VR because it consists of several forward/backprojection steps and a whole optimization routine.

B. Quantitative Results: Phantom Data

For the dynamic phantom data the 3-D error and a quantitative 3-D image metric can be evaluated. In order to measure only the artifacts introduced by the heart motion, the non-gated FDK reconstruction using all projections of the static heart phantom of the same heart phase is used as gold standard. The error as well as the image quality metric were evaluated inside a mask around the ventricle. The relative root mean square (rRMSE) was used to quantify the 3-D reconstruction error [15]. As a 3-D image quality metric the universal image quality index (UQI) was computed [15]. The UQI ranges from -1 to 1, with 1 as the best overlap between both reconstructions. The results at two different relative heart phases (30%, 80%) are given in Table I. All three motion compensated reconstructions achieve comparable results, and the image quality improved with respect to the initial images.

Table I: The rRMSE and the UQI of the dynamic phantom model for heart phases 30% and 80%. The best values are marked in bold.

30%	rRMSE	UQI	80 %	rRMSE	UQI
FDK-VR$_r$	**0.09**	**0.98**	FDK-VR$_r$	**0.06**	**0.99**
FFDK-VR$_r$	**0.09**	**0.98**	FFDK-VR$_r$	**0.06**	**0.99**
F-VR$_r$	**0.08**	**0.98**	F-VR$_r$	**0.06**	**0.99**
FDK-VR	0.15	0.95	FDK-VR	0.12	0.96
FFDK-VR	0.12	0.97	FFDK-VR	0.08	0.98
F-VR	0.11	0.97	F-VR	0.08	0.98
Non-gated FDK	0.15	0.96	Non-gated FDK	0.08	0.97

C. Visual Inspection

The results of the phantom data are presented in Figure 1. The ground truth at a heart phase of 80% is illustrated in Figure 1a. The non-gated FDK reconstruction has motion blur around the left ventricle and the myocardial wall is hardly visible (Fig. 1b). In Figure 1c, the FDK-VR depicts the myocardial wall, but is severely degraded by noise and streak artifacts. The FFDK-VR and F-VR have less streak artifacts and a lower noise level, but have a smoother image impression (Fig. 1e and 1g). All three motion compensated reconstructions show comparable and good delineation of the left ventricle (Fig. 1d, 1f and 1h). The results of the porcine data in Figure 2 illustrate that the non-gated FDK reconstruction averages over all heart phases, as highlighted by the doubled catheter and blurred endocardium edges (Fig.2a). The FDK-VR displays the sharp contours of the endocardium, however prominent streak artifacts are apparent (Fig.2c). A better result is provided by the FFDK-VR and F-VR reconstruction (Fig. 2e, 2g). However, both exhibit blurred streak artifacts and are severely smoothed. The motion compensated reconstructions yield the best results (Fig. 2d, 2f and 2h).

D. Edge Response Profiles

The edge response functions of the different volumes are illustrated in Figure 3. The edge response profile is computed as mean edge profile of the lines indicated in Figure 2. It can be seen that the non-gated FDK reconstruction blurs the edge between the endocardium and the epicardium. The three registration approaches achieve a reasonably good edge profile.

V. Conclusion

We have presented cardiac motion estimation from initial 3-D volume data sets with a deformable B-spline registration. Using motion compensation, the reconstructed image quality is improved compared to the initial image reconstructions. Despite the noise and streak artifacts of the initial images, estimation of a useful motion field is possible. For this image acquisition, non of the presented approaches to enhance the image quality is necessary. This enormously reduces the computational complexity of the framework for dynamic cardiac reconstructions with a C-arm CT system.

Disclaimer: The concepts and information presented in this paper are based on research and are not commercially available.

References

[1] G. Lauritsch, J. Boese, L. Wigström, H. Kemeth, and R. Fahrig, "Towards cardiac C-arm computed tomography," *IEEE Transactions on Medical Imaging*, vol. 25, no. 7, pp. 922–934, July 2006.

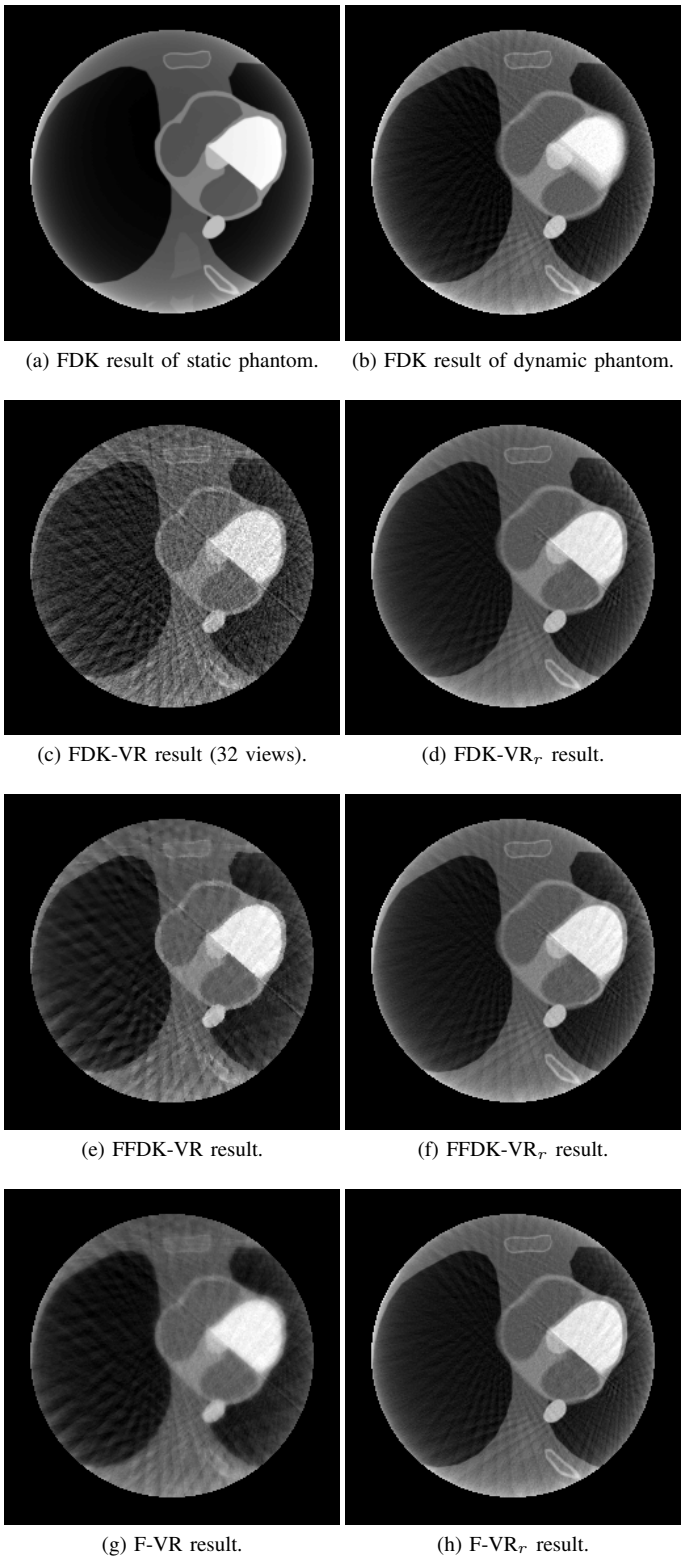

(a) FDK result of static phantom. (b) FDK result of dynamic phantom.

(c) FDK-VR result (32 views). (d) FDK-VR$_r$ result.

(e) FFDK-VR result. (f) FFDK-VR$_r$ result.

(g) F-VR result. (h) F-VR$_r$ result.

Figure 1: Central slice of initial volumes and motion compensated reconstructions of a phantom model and a relative heart phase of $\approx$ 80%.

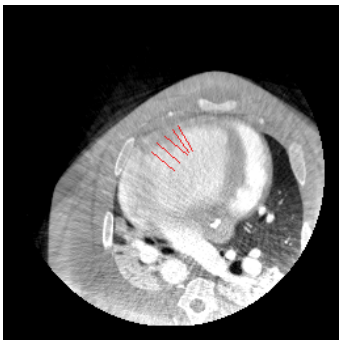

(a) FDK reconstruction.

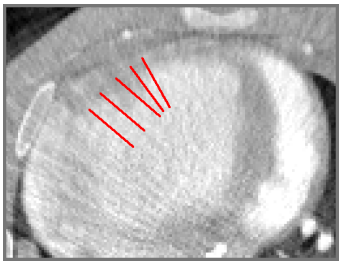

(b) Zoomed line profiles.

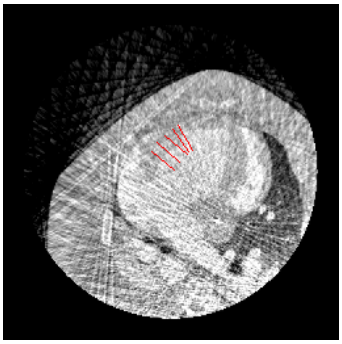

(c) FDK-VR result (32 views).

(d) FDK-VR$_r$ result.

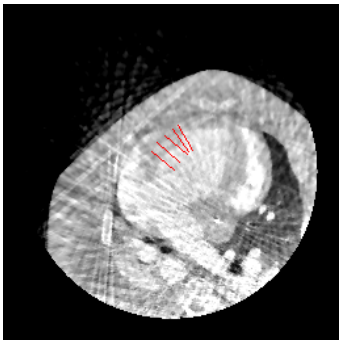

(e) FFDK-VR result.

(f) FFDK-VR$_r$ result.

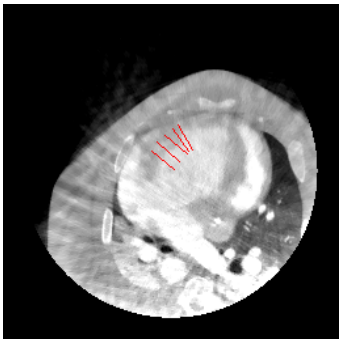

(g) F-VR result.

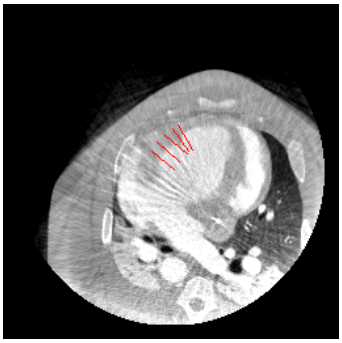

(h) F-VR$_r$ result.

Figure 2: Central slice of initial volumes and motion compensated reconstructions of a porcine model and a relative heart phase of $\approx$ 30% (W 1630 HU, C 50 HU, slice thickness 1 mm).

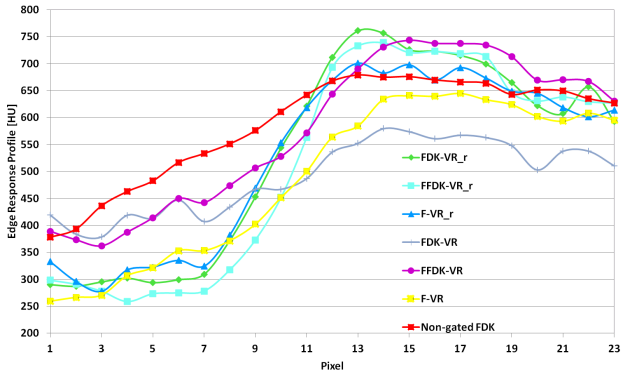

Figure 3: Averaged edge response profile for porcine data of the different algorithms and at 30% heart phase.

[2] A. Isola, M. Grass, and W. Niessen, "Fully automatic nonrigid registration-based local motion estimation for motion-corrected iterative cardiac CT reconstruction," *Med. Phys.*, vol. 37, no. 3, pp. 1093–1109, March 2010.

[3] J. Cammin, P. Khurd, A. Kamen, Q. Tang, K. Kirchberg, C. Chefd Hotel, H. Bruder, and K. Taguchi, "Combined motion estimation and motion compensated fbp for cardiac CT," in *11th International Meeting on Fully Three-Dimensional Image Reconstruction in Radiology and Nuclear Medicine*, 2011, pp. 136–139.

[4] M. Prümmer, J. Hornegger, G. Lauritsch, L. Wigström, E. Girard-Hughes, and R. Fahrig, "Cardiac C-Arm CT: A unified framework for motion estimation and dynamic CT," *IEEE Trans. Med. Imaging*, vol. 28, no. 11, pp. 1836–1849, November 2009.

[5] S. De Buck, D. Dauwe, J.-Y. Wielandts, P. Claus, C. Koehler, Y. Kyriakous, S. Janssens, H. Heidbuchel, and D. Nuyens, "A new approach for prospectively gated cardiac rotational angiography," in *Proc. of SPIE Med. Imag. 2013*, vol. 8668, 2013, p. 86682W.

[6] K. Müller, C. Rohkohl, G. Lauritsch, C. Schwemmer, H. Heidbüchel, S. De Buck, D. Nuyens, Y. Kyriakou, C. Köhler, and J. Hornegger, "4-D motion field estimation by combined multiple heart phase registration (CMHPR) for cardiac C-arm data," in *Proc. of the IEEE NSS / MIC, 2012*, 2012.

[7] C. Rohkohl, G. Lauritsch, A. Nöttling, M. Prümmer, and J. Hornegger, "C-arm CT: Reconstruction of dynamic high contrast objects applied to the coronary sinus," in *Proc. of the IEEE NSS / MIC, 2008*, Dresden, October 2008.

[8] C. Tomasi, "Bilateral filtering for gray and color images," in *Proc. of the IEEE Int. Conf. on Comp. Vis.*, 1998, pp. 839–846.

[9] G.-H. Chen, J. Tang, and S. Leng, "Prior image constrained compressed sensing (PICCS): A method to accurately reconstruct dynamic CT images from highly undersampled projection data sets," *Med. Phys.*, vol. 35, no. 2, pp. 660–663, February 2008.

[10] L. Ritschl, F. Bergner, C. Fleischmann, and M. Kachelrieß, "Improved total variation-based CT image reconstruction applied to clinical data," *Phys. Med. Biol.*, vol. 56, no. 6, pp. 1545–1562, Februar 2011.

[11] S. Klein, M. Staring, K. Murphy, M. Viergever, and J. Pluim, "elastix: a toolbox for intensity based medical image registration," *IEEE Trans. Med. Imaging*, vol. 29, no. 1, pp. 196–205, 2010.

[12] D. Schäfer, J. Borgert, V. Rasche, and M. Grass, "Motion-compensated and gated cone beam filtered back-projection for 3-D rotational x-ray angiography," *IEEE Trans. Med. Imaging*, vol. 25, no. 7, pp. 898–906, July 2006.

[13] W. Segars, M. Mahesh, T. Beck, E. Frey, and B. Tsui, "Realistic ct simulation using the 4D XCAT phantom," *Med. Phys.*, vol. 35, no. 8, pp. 3800–3808, August 2008.

[14] A. Maier, H. Hofmann, C. Schwemmer, J. Hornegger, A. Keil, and R. Fahrig, "Fast simulation of X-ray projections of spline-based surfaces using an append buffer," *Phys. Med. Biol.*, vol. 57, no. 19, pp. 6193–6210, October 2012.

[15] P. Theriault-Lauzier, J. Tang, and G.-H. Chen, "Prior image constrained compressed sensing: Implementation and performance evaluation," *Med. Phys.*, vol. 39, no. 1, pp. 66–80, January 2012.